Proceedings World Geothermal Congress 2026
Calgary, Canada, June 8 – 11, 2026

# Novel Pressure Recovery System for Increasing Efficiency of Geothermal Power Plants

Azam Thatte[1]*, Doug Simpkins[2], Mauricio Rivas[2], Lev Ring[2] and Cindy Taff[2]
Energy Recovery. Inc.[1]*, Sage Geosystems[2]
athatte@energyrecovery.com

**Keywords:** Pressure Geothermal Systems, Rotary Pressure Exchanger, Efficiency, Pressure Recovery, Hydraulic Energy, Supercritical CO2 Power Cycle, Binary Power Plant

## ABSTRACT

Compared to the traditional Enhanced Geothermal Systems (EGS), the Pressure Geothermal Systems (PGS) reduce the water circulation impedance through the subsurface system. In PGS, the pressure-propped fractures are used to keep flow impedance low and have subsurface above the fracture opening pressure at all times, which improves the hydro-mechanical performance of the geothermal system. However, high differential pressure re-injection pump is required in such a PGS, which adds a significant parasitic load and reduces efficiency and net power output from the geothermal power plant. To remedy this issue, this paper presents a novel pressure recovery system using Rotary Pressure Exchanger (RPX) to recover up to 95% of the pressure energy from PGS well and utilize it to pressurize the brine going into the re-injection well. RPX has a high speed axially ducted rotor that receives the low pressure, low temperature re-injection fluid and the high pressure, high temperature fluid from the production well. As the duct rotates, it is alternately exposed to the low and high pressure RPX ports, and through a direct fluid-to-fluid contact pressure exchange, the pressure energy from production fluid is transferred to the reinjection fluid. This pressure recovery significantly reduces the high pressure reinjection pump work and associated parasitic losses of the geothermal power plant. This paper presents a novel pressure recovery system design for a PGS geothermal power plant utilizing RPX. Fundamental physical mechanisms governing RPX are outlined. The performance characteristics and efficiency improvement of RPX integrated PGS binary power plant are quantified.

## 1 INTRODUCTION

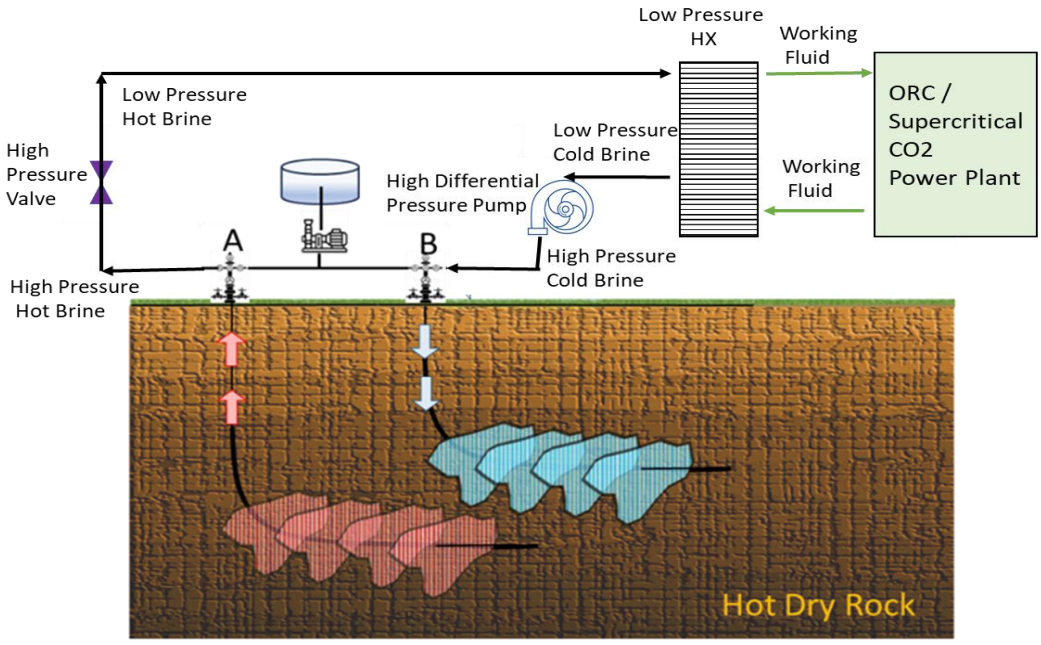



**Figure 1. Pressure Geothermal System (PGS) with a non-connected subsurface. Huff-n-Puff type operation moves a fraction of the hot pressurized fluid from one well to another to extract heat.**

Pressure Geothermal Systems (PGS) is a type of hot dry rock (HDR) technology with a single-well pair approach (i.e. wells do not connect in the subsurface) as opposed to the traditional Enhanced Geothermal Systems (EGS)

in which wells are connected in the subsurface via fractures. Figure 1 shows a PGS with two wells with non-connected fracture system moving only a small portion of fluid from Well A fractures to the power plant and subsequently re-injecting into Well B fractures; after a pre-defined time, the flow of fluid is reversed so that the fluid volumes are brought to the original state and thus completing a full cycle of the Huff-n-Puff operations; the fracture systems are maintained open by fluid pressures above the minimum in-situ stress but below the threshold that would induce further propagation so that no proppants are used. Details on the thermal migration dynamics occurring at the fracture level of PGS can be found in Rivas et al. (2025).

Earlier in Rivas et al. (2024), it was shown that the PGS design drastically reduces system impedance, a measure of flow resistance of the moving fluid, and reduces parasitic energy losses (power lost to the pump injecting fluid into the subsurface system). Moreover, the single-well pair approach of PGS, i.e. well/fracture design and operation, takes advantage of Oil and Gas (O&G) techniques and commercially available technology that may be deployed worldwide.

This paper introduces and analyzes a novel device called Rotary Pressure Exchanger (RPX) that forms part of the high-pressure power plant seen in Fig. 1 and allows the effective utilization of high-pressure energy at surface to reduce the re-injection pump power consumption and enables the economic/scale-up viability of PGS.

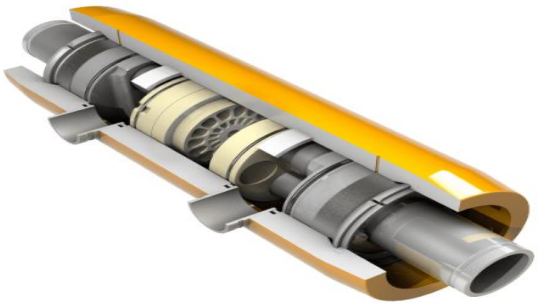
Section 2 describes the design and working principles of the RPX device. Section 3 discusses an example implementation of the RPX in a PGS power plant consisting of supercritical CO2 (sCO2) power cycle. Results from 3D flow dynamics and species transport model of RPX are presented. Preliminary results for the key performance variables like power plant efficiency, sCO2 turbine power output, sCO2 compressor power input needed, the thermal delivery required from PGS and their sensitivity to power plant's gas cooler exit temperature ( influenced by ambient temperature) are provided. Finally the re-injection pump power saved by RPX in above PGS powered sCO2 power plant and its implications on the PGS techno-economics are discussed.

## 2 ROTARY PRESSURE EXCHANGER (RPX)

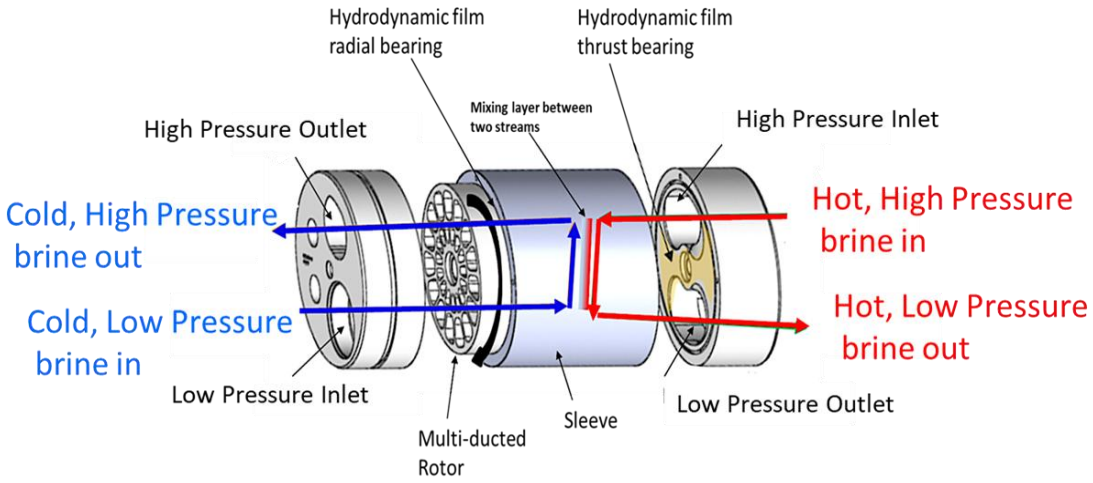
A novel device called rotary pressure exchanger (RPX) [Thatte 2019] is recently being developed to perform pressure recovery from high pressure geothermal brine and use this pressure for re-injecting the low pressure, low temperature brine back into the subterranean system. This section describes the design and working principle of RPX.

### 2.1 Design of RPX

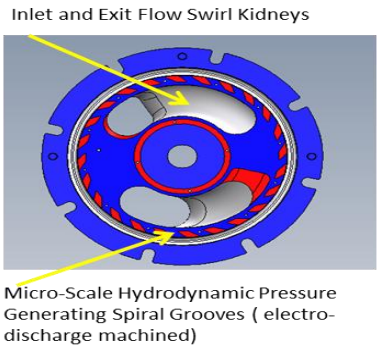
Figure 2(a) shows the design of the RPX device. There is a rotor with multiple ducts spinning inside a sleeve (Fig. 2(b)). The two end covers, shown as HP-in end cover and LP-in end cover form the entry and exit passages for the motive fluid and the process fluid. Here, HP-in = high pressure motive fluid inlet, LP-in= low pressure process fluid inlet that needs to be pressurized, HP-out = high pressure process fluid obtained as a result of pressure exchange between motive fluid and process fluid, LP-out = low pressure motive fluid rejected out of the system. The entrance ports in the end covers can have a special shape in the form of a kidney (e.g. see Fig. 2(b) right end cover) that helps direct the flow with a specific swirl angle into the rotor. This helps generate optimal hydraulic torque that drives the rotor. Rotor is hydraulically driven by the momentum change of the high pressure fluid entering into rotor through the end covers. Carefully designed ramp angles in end covers that change direction of the incoming flow (both HP-in & LP-in) achieve such a momentum change. A shaft can be attached to the rotor to couple it with a motor, for example, to drive the rotor at higher speeds than that can be achieved by pure flow momentum or to slow the rotor down to an optimal speed in case there is excessive hydraulic torque being generated by the incoming fluid streams. However it must be noted that the motor torque and motor power consumed is negligible compared to the hydraulic torque generated by incoming fluid stream and hence motor is not the primary source of energy driving RPX. The hydraulic torque imparted to the rotor by the HP-in and LP-in fluid streams as they swirl through the end covers produces self-sustaining rotary motion of the RPX rotor.



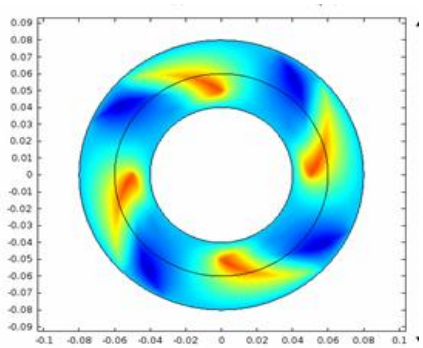
(a)




(b)




(c)



(d)

**Figure 2. (a) RPX cutaway section. (b) Core of the RPX consisting of an axially ducted high speed rotor, sleeve and the two axial end caps.**

RPX rotor spins inside the annular sleeve separated by a few micron radial clearance. The radial clearance is not constant but has a profile that generates hydrostatic pressure distribution on the outer surface of the rotor along the length of the rotor. This clearance profile not only acts as a seal but also as a radial bearing keeping rotor freely spinning inside the sleeve and resists any tilt in the rotor. Additionally, the rotor is separated from the two end covers by an axial gap of only a few microns and micro-scale spiral grooves ( Fig. 2(c)) are machined onto the axial face of the RPX rotor. As the rotor spins, these micro-scale spiral grooves generate hydrodynamic pressure lift (Fig. 2 (d)) in the thin micro-scale fluid film and act as an axial thrust bearing to provide a resisting

force against rotor motion towards the end covers. This force progressively increases as the rotor approaches the end covers and the micro-scale fluid film becomes increasingly stiffer. This increased stiffness of the fluid film prevents rotor from coming into contact with the end covers and avoids any rubs during high pressure, high speed operation of RPX.

### 2.2 Working Principle of RPX

Figure 3 shows the working principle of RPX. Rotation of the rotor provides alternating hydraulic communication of the fluid in the rotor duct exclusively with an incoming high pressure fluid (HP-in motive flow) from the kidney shaped port in one of the end covers and then a very short interval (few milliseconds) later, exclusively with an incoming low pressure fluid (LP-in process flow) from kidney shaped port in the opposite end cover. As a result, axially counter-current flow of fluid is alternately achieved in each duct of the rotor, creating two discharge streams, a reduced pressure motive fluid stream (hot geothermal brine in this case) and an increased pressure process fluid stream ( re-injection fluid stream in this case)..

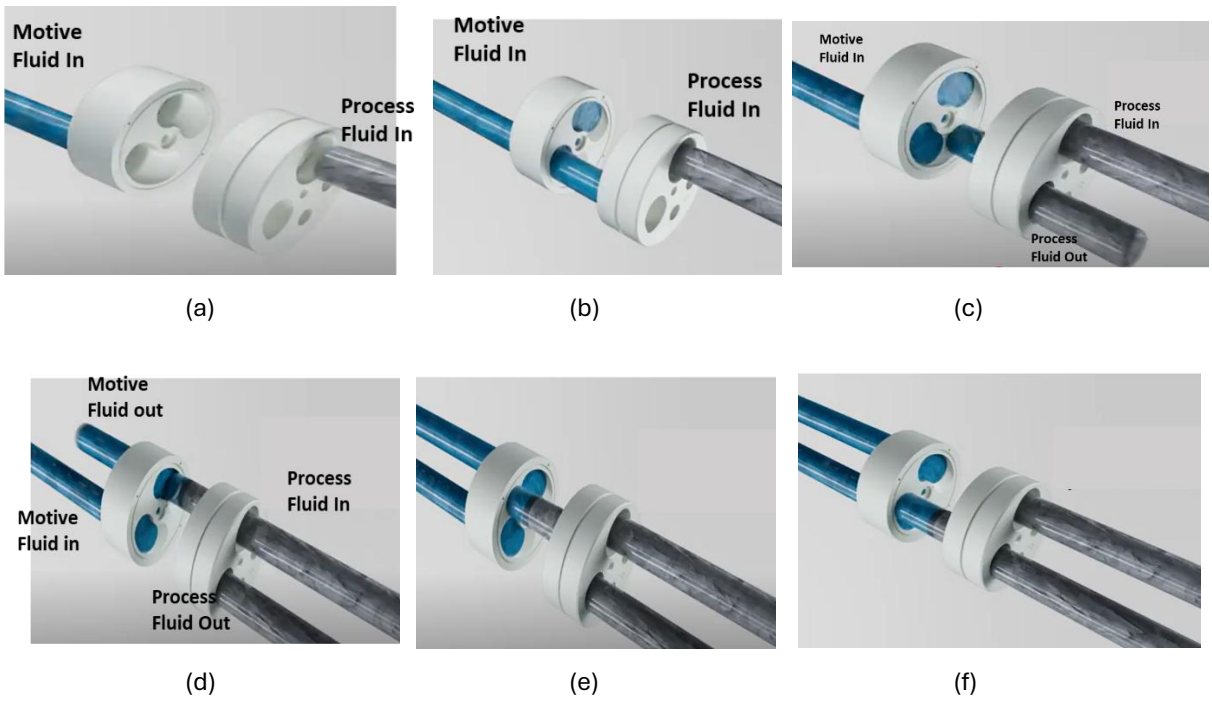



**Figure 3. Sequence of steps (a-f) demonstrating interaction between motive fluid stream and process fluid stream within an RPX rotor duct (multiple such ducts in the rotor).**

Figure 3 (a-f) show the sequence of steps happening inside RPX. The high pressure motive fluid (blue stream) enters the RPX rotor through HP-in port and drives out the plug of high pressure process fluid (grey plug of fluid), that was pressurized from previous step, through HP-out port ( steps a-c). As the duct continues rotation, the high pressure motive fluid then gets sealed between two sealing faces at axially opposite ends of the rotor. Then as the duct gets exposed to the low pressure LP-out port, an acoustic wave de-pressurizes the duct and ejects the high pressure motive fluid plug from the duct into the low pressure LP-out port (step d). This is followed by the duct exposure to LP-in port, which is circumferentially clocked and delayed with respect to the LP-out port. The process fluid then enters the duct through LP-in port and forces the low pressure motive fluid in the duct (blue plug of fluid) out of the LP-out port (step d). Then as the duct continues rotation and the process fluid gets sealed between axially opposite faces. As the duct continues rotation further, it is exposed to the high pressure HP-out port and an acoustic wave pressurizes the process fluid plug to almost the same pressure as the high pressure motive fluid stream (step e). The duct continues its rotation further and gets exposed to the high pressure HP-in port, which is circumferentially clocked and delayed with respect to the HP-out port. HP-in fluid stream then enters the duct and forces the high pressure process fluid plug out of the HP-out port (step f). This completes one rotation of the RPX rotor and one full cycle of pressurization of process fluid stream and

depressurization of motive fluid stream. This cycle repeats several hundred times a minute as the rotor spins at high speed.

The level of mixing between the two fluid streams in the duct is minimal because each duct has a diffusion layer (shown by dark strip in Fig. 3 (e, f)) that serves as a buffer zone between the two fluid streams that enter and exit from opposite end covers. This permits the high pressure motive fluid to transfer its pressure to the incoming low pressure process fluid stream without significant mass mixing.

The rotor spins inside a sleeve and its flat end faces are separated from the faces of the end cover by a few microns thick gap. The gap on the HP-in end cover side is occupied by the motive fluid film that acts both as a film riding thrust bearing and a seal. The gap on the LP-in end cover side is occupied by the process fluid film and acts as a thrust bearing and a seal on the other side. The gap between rotor and sleeve is also few microns in radial thickness and acts as a journal bearing. As described above, the micro-scale hydrodynamic features like spiral grooves are designed on the axial face of the rotor to provide high load carrying capacity and optimal stiffness and damping characteristics to the bearing film. RPX has a fairly low length to diameter ratio for the rotor bearing system. Additionally, the entire rotor is encased in a sleeve with a micron scale fluid film in the annular gap between rotor & sleeve that provides it a large radial bearing surface and hence provides good stiffness and damping characteristics. This helps the rotordynamic stability of RPX. In addition, the rotor system shown here also has low cross-coupled stiffness and positive damping characteristics. Above design feature help mitigate the rotordynamic stability challenges.

## 3 RPX INTEGRATED PRESSURE GEOTHERMAL SYSTEM WITH SUPERCRITICAL CO2 POWER PLANT

When identifying the right choice for thermal to mechanical power conversion in a PGS system, the unique properties of supercritical CO2 translate into several distinct advantages as follows:

i) Reduced Compression Work: A primary thermodynamic advantage stems from the ability to operate the compressor near the pseudo-critical line. In this region, small changes in temperature or pressure cause significant shifts in sCO2 density, allowing for a substantial reduction in the energy required for compression compared to ideal gases or traditional steam cycles [Musgrove et.al. 2017]. This directly and significantly increases the net thermal-to-electric energy conversion efficiency.2 The efficiency advantage of sCO2 is not solely due to its supercritical state, but critically, its ability to leverage the pseudo-critical region for highly efficient compression. This allows the compressor to operate with a fluid that has a liquid-like density, dramatically reducing the energy required for compression compared to compressing a gas. This means that for a given amount of heat input, a much larger proportion can be converted into useful work because less energy is wasted in the compression phase. This characteristic is particularly crucial for lower-grade heat sources, where the overall energy available for conversion is already limited, making them more commercially attractive. This implies a design philosophy that actively seeks to operate the compressor near this pseudo-critical point for maximum benefit.

ii) High Thermal Efficiency: The elevated fluid density, high specific heat capacity, and the absence of a phase change (unlike steam cycles) contribute to higher overall thermal efficiencies for sCO2 cycles. For instance, efficiencies for industrial waste heat recovery applications can reach up to 27.9%.

iii) Exceptional Compactness and High Power Density: The high density of sCO2, particularly near its critical point, enables the design of much smaller and more compact turbomachinery (turbines and compressors) and heat exchangers. This results in a higher power output for a turbine of similar size, leading to smaller, lighter, and potentially cheaper power generation systems. This compactness reduces the environmental footprint and construction costs of new facilities.

iv) Simpler Cycle Layout: sCO2 cycles can offer a simpler overall plant layout compared to the multi-stage and complex steam Rankine cycles, especially those requiring multiple turbine stages and associated casings.

v) Wide Adaptability to Low Grade Heat Sources: While the "moderate-temperature" range of 350 deg. C-800 deg. C is where supercritical CO2 Brayton cycle's peak performance is observed, its competitive performance extends to significantly lower temperatures. sCO2 cycles are highly versatile and can be effectively integrated with low grade heat sources. CO2 as a working fluid possesses a very high thermal resistance. This enables its application across a wide operating temperature range, including lower temperatures such as 200°C for

geothermal applications. This versatility is crucial for effectively tapping into the vast low-grade geothermal resource base. For geothermal power plants, thermodynamic cycle efficiencies exceeding 10% can be attained with the supercritical Brayton cycle, outperforming transcritical CO2 Rankine cycles. The efficiency advantage of sCO2 at 200°C suggests that sCO2 can unlock geothermal resources that are too cool for traditional steam cycles and where Organic Rankine Cycle (ORC) efficiency plateaus, making previously marginal resources economically viable.

vi) Reduced Water Consumption and Dry Cooling Potential: A critical advantage of sCO2 Brayton cycles, especially pertinent for geothermal applications often located in water-stressed regions, is their ability to operate without requiring water for phase change, unlike conventional steam cycles. In such plants, the sCO2 power cycle operates with dry gas cooler exchanging heat directly with ambient air. This makes them ideal for areas with water scarcity or where water usage is restricted. Dry cooling, which uses air as the cooling medium, is more readily and efficiently implemented with gas cycles like sCO2 than with steam cycles. The adoption of air-cooled condensers in sCO2 cycles can significantly reduce or even eliminate water consumption for cooling, enhancing the sustainability of geothermal power plants in water-limited environments.

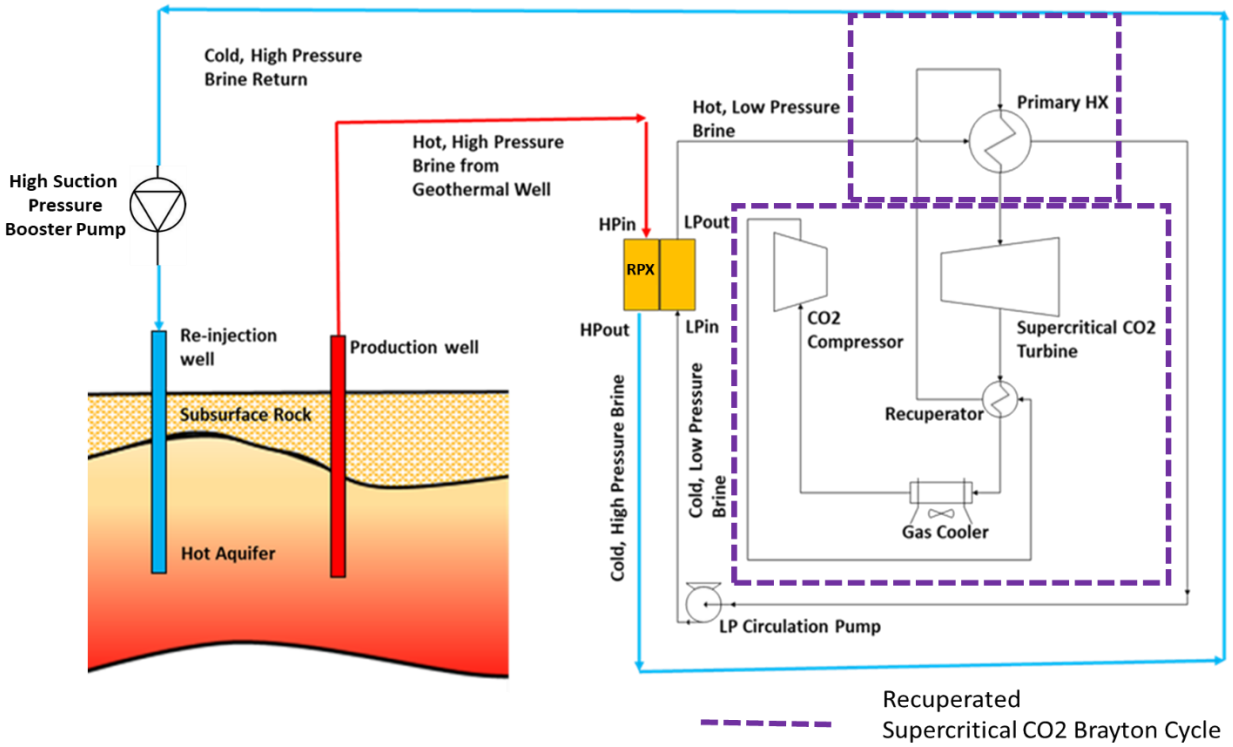


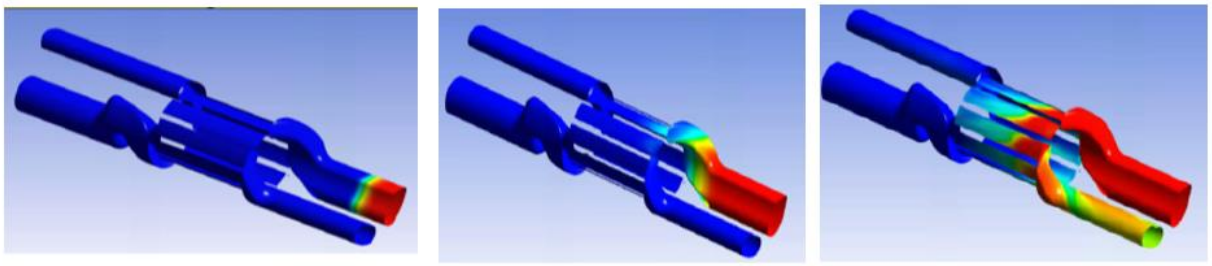

**Figure 4. Pressure geothermal system integrated with RPX and a recuperated supercritical CO2 Brayton power cycle.**

Figure 4 shows such a closed loop, dry cooled, supercritical CO2 Brayton cycle power plant integrated with RPX that uses the geothermal output from PGS. Since in such an sCO2 power cycle, there is still significant amount of enthalpy left at the exit of the turbine, a recuperator is added to exchange heat from turbine exhaust with the compressor discharge stream before geothermal heat is added via the primary heat exchanger. Such a recuperated system is shown in Fig. 4. The hot geothermal brine at 200 bar, 200 deg. C is drawn from the high pressure hot temperature subterranean system. It then enters the high pressure inlet (HPin) port of RPX and exchanges pressure with cold, low pressure (20 bar) brine coming from the binary (supercritical CO2) power plant that needs to be re-injected back into the subterranean system. The hot geothermal brine then exits through the LP-out port of RPX at low pressure (20 bar) but still at high temperature and then proceeds to exchange heat, in the primary HX, with the working fluid (CO2) of the supercritical CO2 power plant. The low pressure, low temperature brine exiting the primary HX of power plant then typically needs to be re-injected back into the subterranean system with a high pressure pump by raising its pressure back to 200 bar, to keep the fractures open. However, now due to pressure exchange within RPX, this 20 bar cold brine stream gets

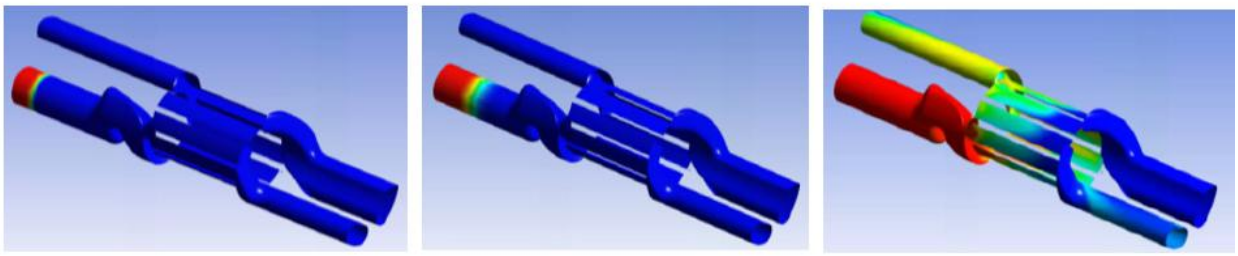
pressurized to 200 bar without consuming any external electrical or mechanical energy, but purely through the pressure-exchange with ( and pressure recovery from) the high pressure hot brine coming out of the production well. This saves a significant amount of pumping power required for re-injection, thus reducing the parasitic load on the power plant and increasing the geothermal plant efficiency and increasing net power output per unit geothermal brine flow. This makes the RPX integrated system techno-economically favorable..

### 3.1 Flow Dynamics & Species-Thermal Transport inside RPX

To evaluate the performance characteristics of RPX in above PGS application, a high fidelity coupled 3D flow, species transport and thermal transport model of RPX is developed. This model is a transient model needed to accurately capture the flow physics occurring during opening & closing of the 10 ducts of the rotor to each of the four ports (HP-in, LP-out, LP-in and HP-out) as the rotor spins.



(a)



(b)

**Figure 5. Results from high fidelity flow dynamics & species transport model of RPX showing RPX is able to achieve pressure recovery without significant mass mixing from the two incoming fluid streams. (a) Species transport from HP-in to LP-out. (b) Species transport from LP-in to HP-out.**

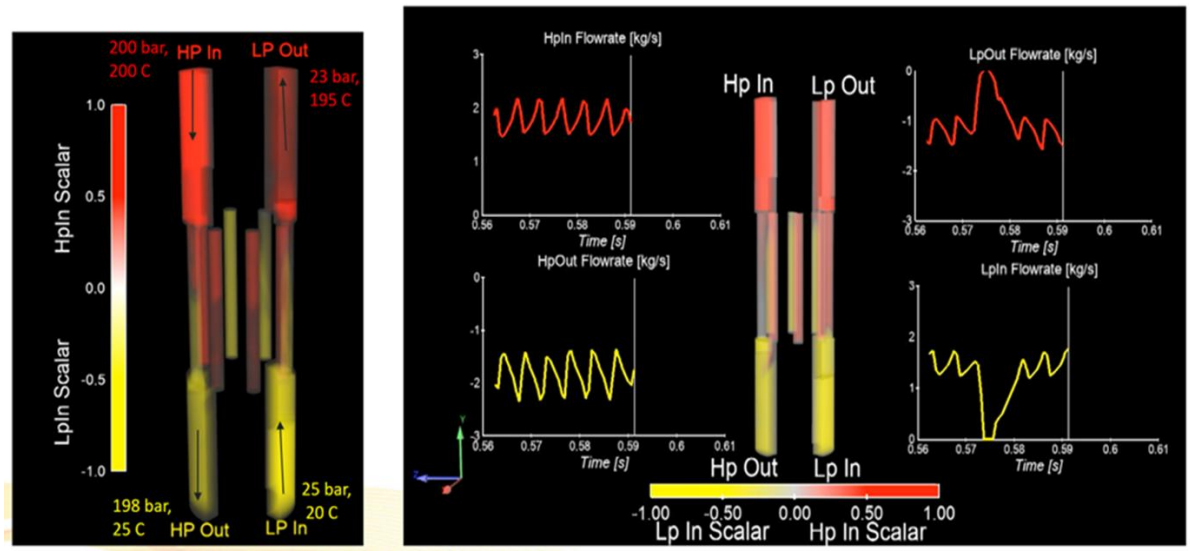


**Figure 6. Tracer injected at both HP-in (red) and LP-inlet (yellow) and their transport tracked through high speed duct rotations. Time evolution of mass flow rates shows that all of the tracer injected at HP inlet exits through LP outlet port and all of the tracer injected at LP inlet port exits through the HP outlet port as desired.**

Two different time scales need to be considered when deciding the resolution of the time step required in the model: i) First one is related to the duct passing frequency, i.e. time it takes for the duct to pass the circumferential extent of the ports in the end covers, where it either receives the fluid from port or ejects the fluid into the port. For examples, at 1200 RPM rotor speed, the duct passing frequency is (1200/60)x10 ducts/rotor = 200 Hz, requiring a time step resolution of at least 10 times that frequency to capture the transient phenomena occurring during passage of the duct. This comes to a time step of 1/ (200*10) = 5E-4 seconds. ii) The second time scale is dictated by the Courant number for the flow through the micron scale gaps driven at high velocities by high pressure differential (~ 200 bar) across the two ports in the end cover. Courant number provides a guideline for estimating the minimum time step required to avoid numerical divergence in the model. Courant Number =Vx $\delta t$ / $\delta x$, where V is the maximum velocity of flow expected through a given mesh element of size $\delta x$ in a given time step $\delta t$. For velocity of the order of 100 m/s through a 10 micron axial gap and to maintain a Courant number < 10, this gives a time step resolution needed for convergence as Dt = 10x10E-6/100 = 1E-6 seconds. The 3D coupled fluid-thermal-species transport model of RPX is developed in ANSYS CFX. It consists of ~ 2 million mesh elements and is solved over 256 parallel cores of a computing cluster. Figures 5, 6 and 7 show some key results from this RPX model.

Figure 5 shows the species transport results from above model. In Fig. 5 (a), shows the concentration of 200 bar, 200 deg. C geothermal brine from the production well entering the HP-in port of RPX, entering the rotating duct and also traversing axially, thus taking a helical path in effect, as the duct spins. Based on the concentration contours seen in the figure, it can be concluded that almost all of this high temperature brine exits through the LP-out port of the RPX and none exits through any of the other two ports. This is exactly as desired for a successful operation. Similarly looking at Fig. 5 (b), it can be seen that almost all of the 25 bar, 20 deg. C cold brine entering the LP-in port makes a U-turn due to the helical path followed during duct rotation and exits through the HP-out port as desired. Hence the model results indicate that there is very little mass-mixing from HP-in to HP-out and from LP-in to LP-out. This is a characteristic of a successful operation of RPX, i.e. achieve pressure recovery without or with very little mass mixing between the two fluid streams.

Figure 6 shows the results from the species transport model where a tracer was injected from both the HP-in port (red tracer) and LP-in port (yellow tracer). The time evolution of these two tracer mass flows is then tracked throughout several rotations of the RPX rotor to infer if any of the red tracer comes out of the HP-out port and if any of the yellow tracer comes out of the LP-out port. Looking from the concentration contours and the mass flow rates of the tracers at the four ports, it can be seen that none of the red tracer exits through the HP-out port and all of it exits through the LP-out port. Similarly, none of the yellow tracer exits through the LP-out port and all of it exits through the HP-out port. This builds the preliminary confidence in the ability of RPX to intake flows of vastly different pressures, exchange their pressures through pressure recovery and route them through correct exit ports.

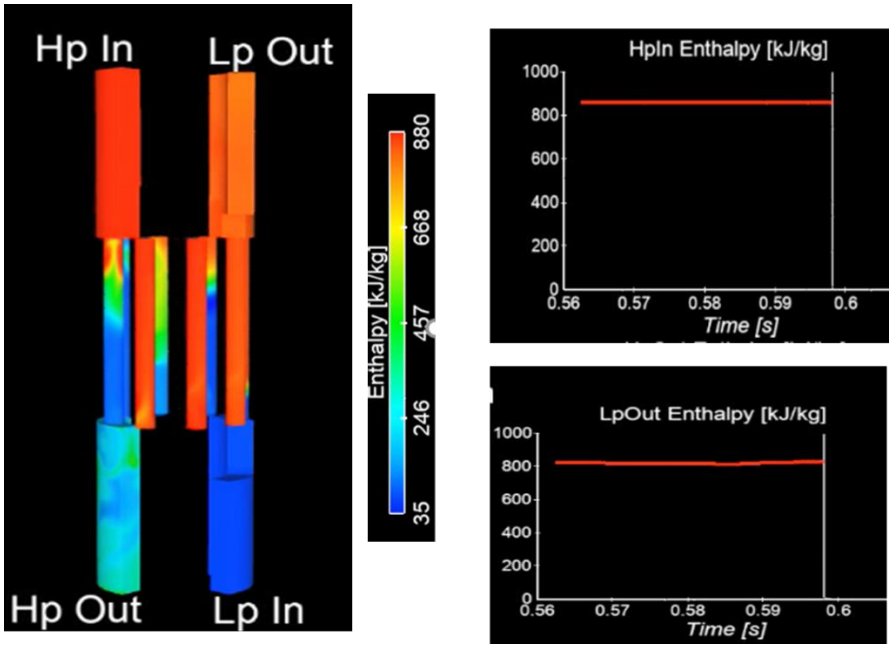
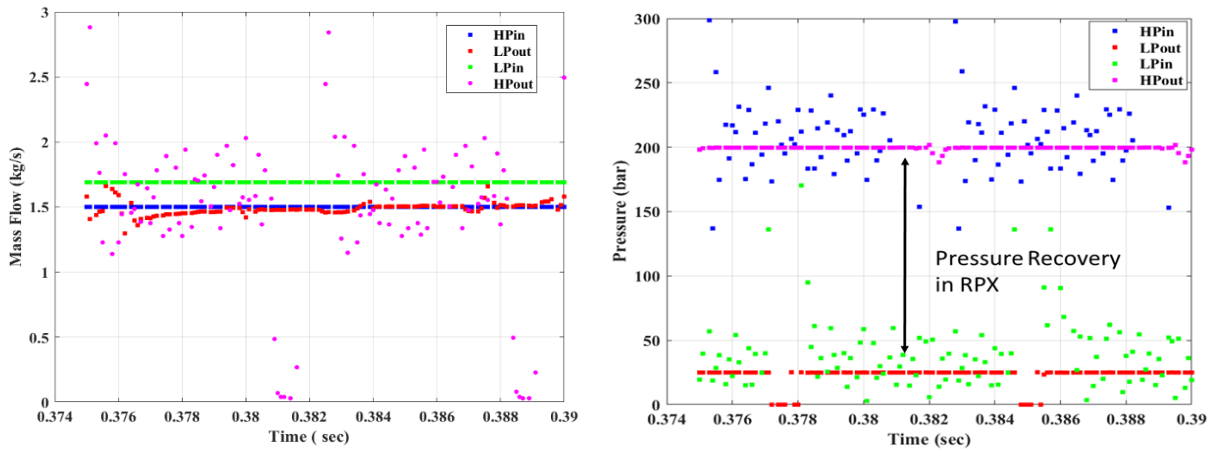



**Figure 7. Enthalpy transport inside RPX rotor ducts. It can be seen that most of the enthalpy entering HPin port is retained at LPout port as desired.**

Figure 7 shows the time evolution of enthalpy transport inside RPX rotor ducts during its high speed operation. It can be observed from the enthalpy contours on the left and the transient plots on the right that most of the high enthalpy entering HPin port of RPX is retained at LPout port. This is a key results, since this high enthalpy provides the thermal input to the heat exchanger of the supercritical CO2 power cycle and thus minimizing the loss of enthalpy from HPin to HPout is important to maintain high efficiency of the combined operation of the well and the power plant.




(a) (b)

**Figure 8. (a) The mass flow analysis from the high fidelity species transport model shows that almost all of the 200 bar, 200 deg. C brine mass flow entering from HPin port of RPX exits through the LPout port at 25 bar as desired. ( compare the blue and the red dots). Also all of the 25 bar, 20 deg. C brine mass flow entering the LPin port exits through the 200 bar HPout port of RPX ( compare the green and the purple dots). Note: there is cyclic variation in exit mass flow during the duct rotation, however on a time averaged basis per rotation, the LPin and HPout mass flows are almost equal. (b) Model shows that RPX is able to recover almost all of the differential pressure between the high pressure geothermal production well brine stream and low pressure re-injection brine stream. Using this pressure recovery RPX is able to pressurize the 25 bar low temperature brine to the 200 bar re-injection pressure required by PGS.**

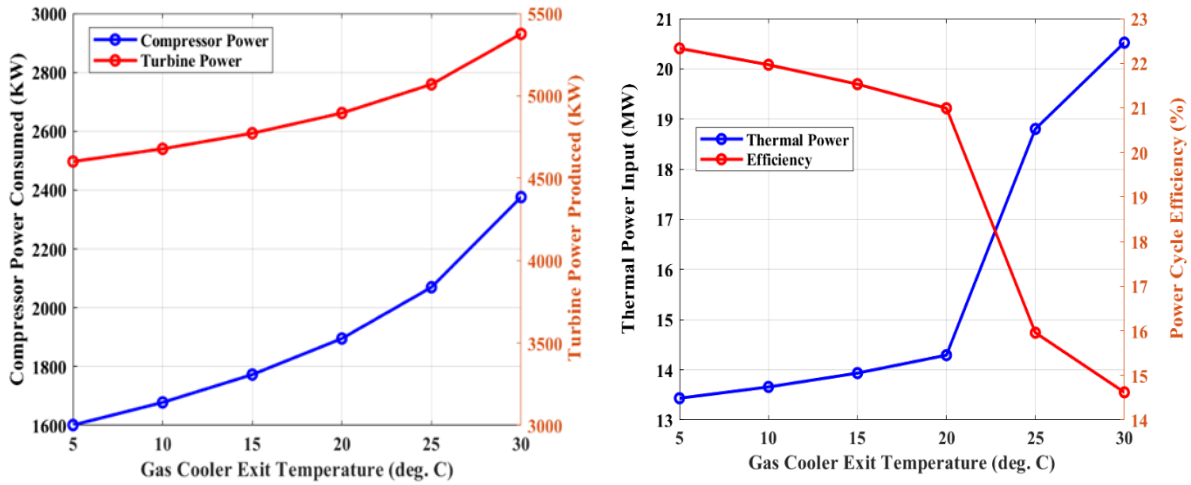
Figure 8(a) shows the time evolution of mass flows at the 4 ports of the RPX during a duct rotation. The desired mass flow boundary condition is specified in the model at the HP-in port (1.5 kg/s) and LP-in port (1.7 kg/s) while the boundary condition pressures are specified at the LP-out ( 25 bar) and HP-out (200 bar) ports. The model then calculates the flows at the two exit ports and predicts the pressures at the two inlet ports. It can be seen that almost all of the 200 bar, 200 deg. C brine mass flow entering from HPin port exits through the LPout port at 25 bar as desired. (compare the blue and the red dots). Also, all of the 25 bar, 20 deg. C brine mass flow entering the LPin port exits through the 200 bar HPout port of RPX ( compare the green and the purple dots). Note that there is cyclic variation in the HP-out mass flow during the duct rotation, however on a time averaged basis per rotation, the LPin and HPout mass flows are similar.

Figure 8(b) shows the time evolution of pressure at the 4 ports of the RPX during a duct rotation. As mentioned above, the boundary condition specified holds the pressure constant at the two exit ports and the model calculates the pressure required at the two inlet ports to allow the mass flows calculated per Fig. 8(a). As can be seen, during the duct rotation, the HP-in and LP-in pressures oscillate around the mean values equal to the pressure at HP-out ( 200 bar) and LP-out (25 bar) respectively. This indicates that RPX is able to successfully boost the pressure of the LP-in stream from 25 bar to 200 bar without consuming any external mechanical or electrical energy. The energy required for this pressure boost comes purely from the hydraulic energy recovered during the pressure drop from HP-in stream to LP-out stream. These results provide initial confidence in the ability of RPX to recover pressure energy from high pressure, high temperature geothermal brine coming out of the production well and use it to pressurize the cold brine needed for re-injection into the re-injection well of PGS.

### 3.2 PGS Power Cycle Analysis

Figure 9 shows the results from analysis of recuperated supercritical CO2 Brayton cycle and highlights the sensitivity of key performance indicators to the CO2 gas cooler exit temperature ( function of ambient temperature). The analysis assumes a geothermal heat input to the CO2 plant from PGS at 200 deg. C and that the sCO2 power plant produces a net 3 MW electrical power output. Figure 9 (a) shows the compression power consumed and turbine power output for this net 3 MW power plant. As can be seen the compression work reduces significantly from 2.4 MW to 1.6 MW if the gas cooler exit temperature is reduces from 30 deg. C to 5 deg. C. Since the net power output of the plant required is the same 3 MW, this reduces the power output required from the turbine from ~5.5 MW to ~4.6 MW.

Figure 9 (b) shows the Efficiency and Thermal power input required for this recuperated sCO2 Brayton cycle to produce net 3 MW output power as a function of gas cooler exit temperature. The sCO2 Brayton power cycle efficiency increases from ~ 14.8 % to 22.5% with reduction in gas cooler exit temperature from 30 deg. C to 5 deg. C. With this increase in cycle efficiency, the heat input to the sCO2 plant required from PGS reduces from 20.5 MW to 13.5 MW. This illustrates the role of gas cooler exit temperature and hence of the ambient temperature in overall techno-economics and levelized cost of geothermal power.



(a) (b)

**Figure 9. : Results from recuperated supercritical CO2 Brayton cycle analysis showing sensitivity to CO2 gas cooler exit temperature ( function of ambient temperature). (a) shows compression power consumed and turbine power output for a net 3 MW power plant. (b) shows thermal input needed from geothermal brine to produce net 3 MW power output.**

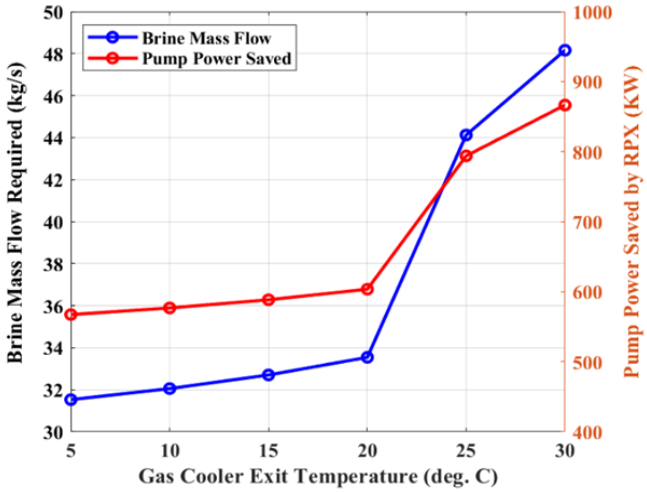



**Figure 10. : Geothermal brine mass flow at 200 deg. C required for a 3 MW net power output from supercritical CO2 power plant. The re-injection pump power saved by RPX to pump this brine flow back into the aquafer is also shown.**

Figure 10 shows the variation of geothermal brine mass flow at 200 deg. C required for a 3 MW net power output as a function of gas cooler exit temperature of sCO2 power plant. The hot brine flow required drops from 48 kg/s to 32 kg/s as gas cooler exit temperature reduces from 30 deg. C to 5 deg. C.

Next, the analysis on PGS side is conducted to calculate the energy required to pump the cold low pressure brine flow coming from sCO2 power plant's primary heat exchanger back into re-injection well. Also the analysis is conducted to evaluate the hydraulic pumping work performed by RPX onto this 25 bar, 20 C brine using the pressure recovery achieved within the RPX. The net re-injection pumping power saving theoretically achievable using RPX is shown in Fig. 10 (red curve). This energy saving is primarily due to elimination of re-injection pump work due to pressure recovery in RPX as demonstrated in Fig. 8(b) above. The re-injection power saved ranges between 900 KW at 30 deg. C CO2 gas cooler exit temperature to 600 KW at 5 deg. C gas cooler exit temperature. This constitutes energy savings of 30% of the net Geothermal power output of 3 MW for an ambient temperature of 30 deg. C and 20% of the net power output for an ambient temperature of 5 deg. C. Thus it can be seen that RPX can be a valuable technology to reduce the parasitic power loads on PGS geothermal power plants, to increase their efficiency and to increase the net electrical power output per unit geothermal brine mass flow.

## 4 CONCLUSIONS

Pressure Geothermal systems are an attractive alternative to traditional Enhanced Geothermal Systems in order to reduce the impedance to the water circulation through the subsurface system. The hydro-mechanical performance of a single well pair PGS has been shown to be superior to EGS systems, however, the high differential pressure re-injection pump work adds a significant parasitic load to the system and reduces the power plant efficiency and net power output from the geothermal plant. To remedy this issue, in this paper a Rotary Pressure Exchanger (RPX) is analyzed that can achieve up to 95% pressure recovery from high pressure hot brine produced and use it to pressurize the low pressure cold brine needed for re-injection. This significantly reduces the high pressure reinjection pump power consumption and increases the net power output from the geothermal power plant. High fidelity coupled field flow-thermal-species transport model of RPX is developed

and used to analyze key RPX performance characteristics. The analysis showed that a no-pass through, low mass-mixing operation of RPX can be achieved through optimal design of ducts and port circumferential clocking. Analysis also showed > 95% pressure recovery in RPX thus pressurizing the re-injection fluid stream to full re-injection well pressure without requiring external mechanical or electrical energy. This reduces the parasitic load on PGS plant from 20%-30%. Additionally, the role of supercritical CO2 Brayton cycle in achieving efficient, compact turbomachinery for geothermal power generation is discussed. The sensitivity of compression power, power cycle efficiency and the geothermal heat input required for the plant to CO2 gas cooler exit temperature and hence to ambient temperature is analyzed. Effect of ambient temperature on pumping energy saved by RPX is also quantified. Overall, RPX is shown to be an effective technology to increase the efficiency and net power output per unit geothermal mass flow in PGS based geothermal power plants to make them techno-economically more attractive.

## REFERENCES

Brown, D., Duchane, D.V., Heiken, G. and Hriscu, V.T: Mining the Earth's Heat: Hot Dry Rock Geothermal Energy. *Springer-Verlag,* Berlin Heidelberg, Germany (2012).

Rivas, M.A., McGuire, V., Simpkins, D. and Ring, L.: Geopressured Geothermal Systems: An Efficient and Sustainable Heat Extraction Method, *GRC Transactions*, **Vol. 48** (2024).

Rivas, M.A., Simpkins, D., McGuire, V. and Ring, L.: Dynamics of Thermal Migration in Pressure-Propped Fractures During Huff-n-Puff Operations, Proceedings, 50th Workshop on Geothermal Reservoir Engineering, Stanford University, Stanford, CA, USA (2025).

Thatte A.: Transcritical / Supercritical CO2 Recompression Brayton Cycle using a Novel Rotary Liquid Piston Compressor, *Proceedings of ASME Turbo Expo 2019, GT2019-91088, Phoenix, AZ, USA (2019).*

Musgrove et.al.: *Fundamentals and Applications of Supercritical Carbon Dioxide (SCO2) Based Power Cycles 1st Edition*, Elsevier, Editor: Klaus Brun, Peter Friedman, Rich Dennis (2017).